Comparison of Robustness of Complete Ultrashort Optical Pulse Measurement Techniques

Chen-Shao Hsu, Shang-Da Yang

Institute of Photonics Technologies, National Tsing Hua University, Hsinchu 30013, Taiwan

g9566508@oz.nthu.edu.tw

Abstract: We compare the system robustness of: (a) measurement of electric field by interferometric spectral trace observation (MEFISTO), and (b) frequency- resolved optical gating (FROG), which are two techniques used to retrieve intensity and phase of ultrashort optical pulses. Our simulation shows that MEFISTO is substantially more susceptible to additive noise contamination, thought it can rapidly provide the spectral phase without iteration.

1. Introduction:

Measuring the complex fields of femtosecond pulses is essential in ultrafast signal generation and processing, especially when nearly transform-limited or precisely shaped pulses are involved [1-2]. Among the existing techniques that can deliver intensity and phase of signal pulses, frequency-resolved optical gating (FROG) [3] is especially popular because of its robustness against system noises. An interferometric variation of FROG, namely measurement of electric field by interferometric spectral trace observation (MEFISTO), was recently proposed in [4-5]. The primary advantages of this new scheme over conventional FROG are twofold: (a) the data acquisition uses a collinear configuration, which permits the employment of straight waveguides as highly efficient second-harmonic (SH) converters [6]; (b) it requires no iteration in phase retrieval, and can achieve a much faster update rate. Our goal is to investigate whether MEFISTO and FROG are equally robust against system noises as indicated in the previous literature [4].

2. Theory:

Fig. 1 illustrates the schematic of FROG and MEFISTO measurements. A pulse of complex envelope $E(t)$ and carrier frequency f_0 is sent into a collinear Michelson interferometer to produce a pulse pair with variable delay τ. After passing through a nonlinear crystal, one can measure the τ-dependent SH spectrum to obtain an interferometric trace I^{SHG} in terms of delay τ and frequency f [4]:

$$I^{SHG}(f,\tau)=\left|F_t\left\{[E(t)\exp(j2\pi f_0 t)+E(t-\tau)\exp(j2\pi f_0(t-\tau))]^2\right\}\right|^2 \quad (1)$$

where $F_t\{\}$ stands for Fourier transform with respect to t. By calculating the Fourier transform of eq. (1) with respect to τ, we derive:

$$Y^{SHG}(f,\kappa)=F_\tau\left\{I^{SHG}(f,\tau)\right\} \quad (2)$$

which consists of five spectral components centered at delay frequencies of κ=0, $\pm f_0$, and $\pm 2f_0$. Fig. 2 shows the simulated contour plots of: (a) interferometric trace I^{SHG}, and (b) its Fourier transform Y^{SHG}, by assuming a chirped Gaussian pulse of 100-fs width and 1.55-μm central wavelength ($f_0 \approx$193 THz).

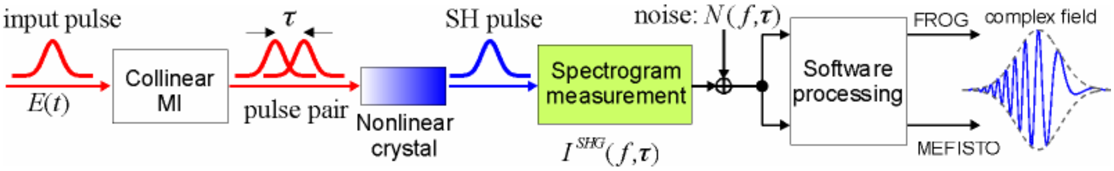

Fig. 1. Schematic of FROG and MEFISTO measurements. MI: Michelson interferometer.

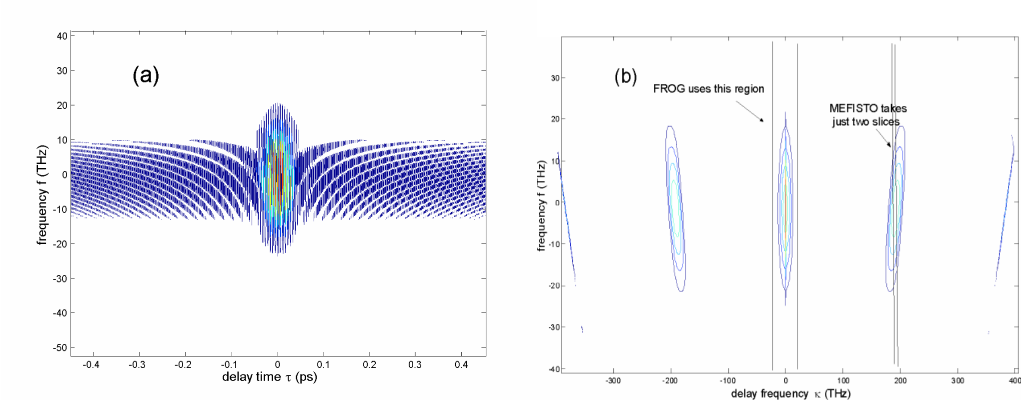

Fig. 2. Simulated contour plots of: (a) interferometric trace $I^{SHG}(f,\tau)$ (where carrier frequency f_0 is subtracted), and (b) its Fourier transform with respect to delay $Y^{SHG}(f,\kappa)$, of a chirped Gaussian pulse.

In FROG measurement, the whole spectral information of Y^{SHG} in the vicinity of κ=0 is extracted for iterative retrieval. However, only two neighboring slices of Y^{SHG} near $\kappa = f_0$ are taken (typically at $\kappa = f_0$, and $f_0 - \Delta f$, where Δf is determined by the size of τ-window) when using MEFISTO to evaluate the spectral phase (see Fig. 2b). The differential spectral phase $\Delta\phi(f) \equiv \phi(f+\Delta f) - \phi(f)$ is of the form [4]:

$$\Delta\phi(f) = \pm\cos^{-1}\left[\Omega(f,\kappa = f_0)\right] \mp \cos^{-1}\left[\Omega(f,\kappa = f_0 - \Delta f)\right] + \phi(0) - \phi(-\Delta f) \tag{3}$$

where $\Omega(f,\kappa) \equiv Y^{SHG}(f,\kappa)/[4U_{SHG}(f)U(f+f_0-\kappa)U(\kappa-f_0)]$, $E(f) \equiv F_t\{E(t)\} = U(f)\exp[j\phi(f)]$, and $E_{SHG}(f) \equiv F_t\{E^2(t)\}$. By choosing an arbitrary reference phase $\phi(0)$, we are able to derive the spectral phase profile $\phi(f)$ by eq. (3).

3. Simulation and Discussion:

We first used a chirped Gaussian pulse of quadratic spectral phase to test the performance of our MEFISTO simulation engine. As shown in Fig. 3, the calculated spectral phase profile $\tilde{\phi}(f)$ agrees well with the exact curve $\phi(f)$. The normalized root-mean-square (RMS) error ε (defined as $\left[\sum_i\left[\tilde{\phi}(f_i) - \phi(f_i)\right]^2 \cdot U^2(f_i) \Big/ \sum_i \phi^2(f_i)\cdot U^2(f_i)\right]^{0.5}$, where the spectral intensity $U^2(f)$ is used as weighting function, and f_i denotes the i-th sampling frequency) is as low as 7.42×10^{-5}, proving the reliability of our simulation codes.

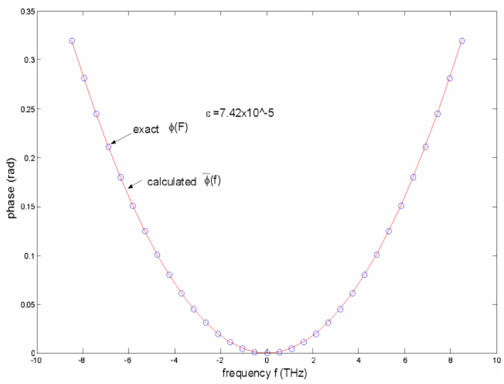

Fig. 3. Exact (circle) and calculated (solid, using MEFISTO) spectral phase profiles of a chirped Gaussian pulse.

We then analyzed the system robustness by adding some random noise to the interferometric trace: $\widetilde{I}^{SHG}(f,\tau) = I^{SHG}(f,\tau) + N(f,\tau)$, where $N(f,\tau) = \delta \cdot u(f,\tau)$, δ is the noise amplitude relative to the peak of $I^{SHG}(f,\tau)$, and $u(f,\tau)$ is implemented by a random matrix uniformly distributed between 0 and 1. The contaminated trace $\widetilde{I}^{SHG}(f,\tau)$ was transformed into $\widetilde{Y}^{SHG}(f,\kappa)$, then properly sampled or filtered to feed our MEFISTO simulation codes or commercial FROG software, respectively. Fig.4 illustrates that the RMS error ε of MEFISTO grows rapidly with noise amplitude δ, and a relatively small noise ($\delta \approx 2\%$) is sufficient to largely degrade the phase retrieval ($\varepsilon \approx 1$). By contrast, Fig. 5 shows that FROG is very insensitive to the additive noise within the range of interest ($\varepsilon = 2.18 \times 10^{-2}$ when $\delta = 2\%$).

Our results can be justified as follows. (a) The noise resistance of FROG mainly comes from the iterative mechanism, which can exclude unrealistic solution corresponding to the noise-contaminated trace [3]. (b) MEFISTO uses far less spectrogram data (pulse information) than FROG, therefore, should be subject to stronger noise problem.

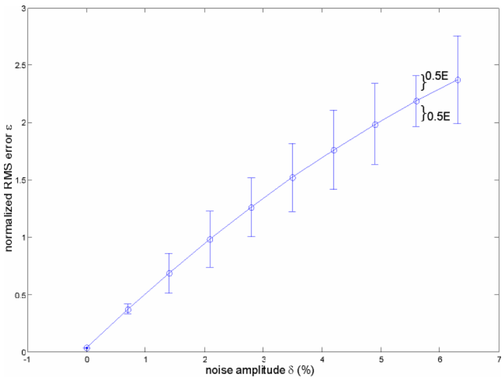

Fig. 4. Noise response of MEFISTO. The length of error bar represents the standard deviation of five data points..

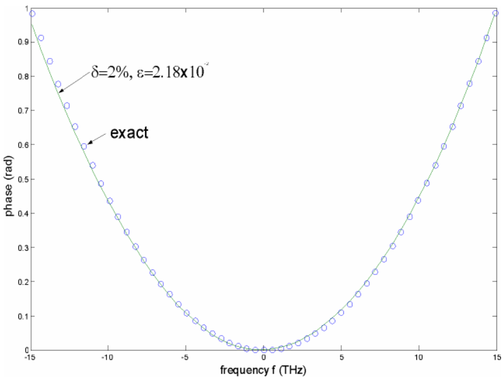

Fig. 5. Exact (circle) and calculated (solid and dashed, using FROG) spectral phase profiles of a chirped Gaussian pulse.

4. Conclusion:

In opposition to [4], our simulation shows that the error-checking capability of MEFISTO is intrinsically inferior to that of FROG for lack of iteration. Its advantage of fast phase retrieval is achieved at the cost of worse system robustness. Employment of additional spectrogram data is expected to improve the noise response of MEFISTO.

References:

[1]. B. C. Thomsen, D. A. Reid, R. T. Watts, L. P. Barry, J. D. Harvey, IEEE Trans. Instrum. Meas. **53**, 186 (2004).

[2]. Z. Jiang, D. S. Seo, S.-D. Yang, D. E. Leaird, R. V. Roussev, C. Langrock, M. M. Fejer, A. M. Weiner, J. Lightw. Technol. **23**, 143 (2005).

[3]. R. Trebino, Kluwer Academic Publishers, Boston, MA, 2000.

[4]. I. Amat-Roldán, I. G. Cormack, P. Loza-Alvarez, D. Artigas, Opt. Lett. **30**, 1063 (2005).

[5]. I. Amat-Roldan, D. Artigas, I. G. Cormack, and P. Loza-Alvarez, Opt. Eepress **14**, 4538 (2006).

[6]. S. -D. Yang, A. M. Weiner, K. R. Parameswaran, M. M. Fejer, Opt. Lett. **30**, 2164 (2005).